J|A|C|S ARTICLES

Published on Web 08/20/2009

Synthesis, Structures, and Electronic Properties of [8Fe-7S] Cluster Complexes Modeling the Nitrogenase P-Cluster

Yasuhiro Ohki,† Motosuke Imada,† Ayuro Murata,† Yusuke Sunada,† Shun Ohta,† Masaru Honda,† Takahiro Sasamori,¶ Norihiro Tokitoh,¶ Motomi Katada,‡ and Kazuyuki Tatsumi*,†

Department of Chemistry, Graduate School of Science and Research Center for Materials Science, Nagoya University, Furo-cho, Chikusa-ku, Nagoya 464-8602, Japan, Institute for Chemical Research, Kyoto University, Gokasho, Uji, Kyoto 611-0011, Japan, and Graduate School of Science and Engineering, Tokyo Metropolitan University, Minami-ohsawa, Hachioji, Tokyo 192-0397, Japan

Received July 4, 2009; E-mail: i45100a@nucc.cc.nagoya-u.ac.jp

Abstract: High-yield synthesis of the iron−sulfur cluster [{N(SiMe$_3$)$_2$}{SC(NMe$_2$)$_2$}Fe$_4$S$_3$]$_2$(μ_6-S) {μ-N(SiMe$_3$)$_2$}$_2$ (**1**), which reproduces the [8Fe-7S] core structure of the nitrogenase P^N-cluster, has been achieved via two pathways: (1) Fe{N(SiMe$_3$)$_2$}$_2$ + HSTip (Tip = 2,4,6-^{i}Pr$_3$C$_6$H$_2$) + tetramethylthiourea (SC(NMe$_2$)$_2$) + elemental sulfur (S_8); and (2) Fe$_3${N(SiMe$_3$)$_2$}$_2$(μ-STip)$_4$ (**2**) + HSTip + SC(NMe$_2$)$_2$ + S_8. The thiourea and terminal amide ligands of **1** were found to be replaceable by thiolate ligands upon treatment with thiolate anions and thiols at −40 °C, respectively, and a series of [8Fe-7S] clusters bearing two to four thiolate ligands have been synthesized and their structures were determined by X-ray analysis. The structures of these model [8Fe-7S] clusters all closely resemble that of the reduced form of P-cluster (P^N) having 8Fe(II) centers, while their 6Fe(II)−2Fe(III) oxidation states correspond to the oxidized form of P-cluster (P^{OX}). The cyclic voltammograms of the [8Fe-7S] clusters reveal two quasi-reversible one-electron reduction processes, leading to the 8Fe(II) state that is the same as the P^N-cluster, and the synthetic models demonstrate the redox behavior between the two major oxidation states of the native P-cluster. Replacement of the SC(NMe$_2$)$_2$ ligands in **1** with thiolate anions led to more negative reduction potentials, while a slight positive shift occurred upon replacement of the terminal amide ligands with thiolates. The clusters **1**, (NEt$_4$)$_2$[{N(SiMe$_3$)$_2$}(SC$_6$H$_4$-4-Me)Fe$_4$S$_3$]$_2$(μ_6-S){μ-N(SiMe$_3$)$_2$}$_2$ (**3a**), and [(SBtp){SC(NMe$_2$)$_2$}Fe$_4$S$_3$]$_2$(μ_6-S){μ-N(SiMe$_3$)$_2$}$_2$ (**5**; Btp = 2,6-(SiMe$_3$)$_2$C$_6$H$_3$) are EPR silent at 4−100 K, and their temperature-dependent magnetic moments indicate a singlet ground state with antiferromagnetic couplings among the iron centers. The ^{57}Fe Mössbauer spectra of these clusters are consistent with the 6Fe(II)−2Fe(III) oxidation state, each exhibiting two doublets with an intensity ratio of ca. 1:3, which are assignable to Fe(III) and Fe(II), respectively. Comparison of the quadrupole splittings for **1**, **3a**, and **5** has led to the conclusion that two Fe(III) sites of the clusters are the peripheral iron atoms.

1. Introduction

Molybdenum nitrogenase consists of two metalloproteins designated as the Fe-protein and the MoFe-protein, and ATP-dependent electron transfer occurs from the Fe-protein to the MoFe-protein, where the catalytic reduction of N_2 takes place.[1] The Fe-protein contains one [4Fe-4S] cubane cluster, while the MoFe-protein has two unusual metal-sulfide clusters, namely the P-cluster and the FeMo-cofactor. The P-cluster is situated between the [4Fe-4S] cluster and the FeMo-cofactor,[2] and is thought to relay electrons from the [4Fe-4S] cluster to the FeMo-cofactor. The P-cluster exhibits multiple oxidation states.[3,4] In the dithionite reduced P^N state, the P-cluster is EPR silent and the Mössbauer spectrum indicates that all iron atoms assume the Fe(II) oxidation state.[5] Redox studies of the P^N state have shown a reversible two-electron oxidation process to form the P^{OX} (P^{2+}) state, while further chemical oxidation with ferricya-

† Nagoya University.
¶ Kyoto University.
‡ Tokyo Metropolitan University.

(1) (a) Burgess, B. K.; Lowe, D. L. *Chem. Rev.* **1996**, *96*, 2983–3011. (b) Howard, J. B.; Rees, D. C. *Chem. Rev.* **1996**, *96*, 2965–2982. (c) *Catalysts for Nitrogen Fixation*; Smith, B. E.; Richards, R. L.; Newton, W. E., Eds.: Kluwer Academic Publishers: Dordrecht, 2004.

(2) (a) Schindelin, H.; Kisker, C.; Schlessman, J. L.; Howard, J. B.; Rees, D. C. *Nature* **1997**, *387*, 370–376. (b) Chiu, H.-J.; Peters, J. W.; Lanzilotta, W. N.; Ryle, M. J.; Seefeldt, L. C.; Howard, J. B.; Rees, D. C. *Biochemistry* **2001**, *40*, 641–650. (c) Schmid, B.; Einsle, O.; Chiu, H.-J.; Willing, A.; Yoshida, M.; Howard, J. B.; Rees, D. C. *Biochemistry* **2002**, *41*, 15557–15565. (d) Tezcan, F. A.; Kaiser, J. T.; Mustafi, D.; Walton, M. Y.; Howard, J. B.; Rees, D. C. *Science* **2005**, *309*, 1377–1380.

(3) (a) Smith, B. E.; Lowe, D. J.; Chen, G.-X.; O'Donnell, M. J.; Hawkes, T. R. *Biochem. J.* **1983**, *209*, 207–213. (b) Hagen, W. R.; Wassink, H.; Eady, R. R.; Smith, B. E.; Haaker, H. *Eur. J. Biochem.* **1987**, *169*, 457–465. (c) Pierik, A. J.; Wassink, H.; Haaker, H.; Hagen, W. R. *Eur. J. Biochem.* **1993**, *212*, 51–61. (d) Tittsworth, R. C.; Hales, B. J. *J. Am. Chem. Soc.* **1993**, *115*, 9763–9797. (e) Spee, J. H.; Arendsen, A. F.; Wassink, H.; Marritt, S. J.; Hagen, W. R.; Haaker, H. *FEBS Lett.* **1998**, *432*, 55–58. (f) Christiansen, J.; Goodwin, P. J.; Lanzilotta, W. N.; Seefeldt, L. C.; Dean, D. R. *Biochemistry* **1998**, *37*, 12611–12623.

 10.1021/ja9055036 CCC: $40.75

Chart 1. Structures of the nitrogenas P^N-cluster and **1**

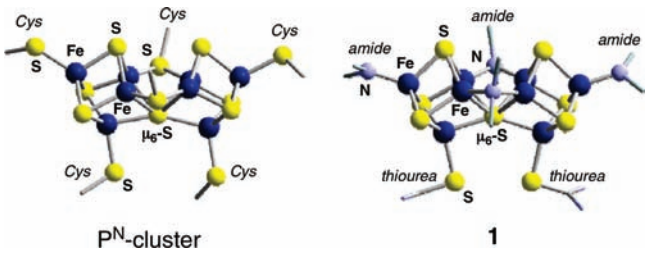

nide or solid thionine gave rise to the $P^{superox}$ (P^{3+}) state.[3b,c] The P^{OX} state exhibits a very weak EPR signal near $g = 12$. On the other hand, the intermediate P^{1+} state was detected by careful redox titration experiments of the P^N-cluster,[3a,d] and shows two sets of EPR signals arising from $S = 1/2$ and 5/2 mixed spin systems.

The high-resolution crystal structures of nitrogenases from *Azotobacter vinelandii* and *Klebsiella pneumoniae* were reported in 1997 and 1999, respectively,[6] and the P-cluster was found to be an [8Fe-7S] core consisting of two [4Fe-3S] incomplete cubane units linked by a six-coordinate sulfur atom (μ_6-S) (Chart 1). The unprecedented cluster structure has presented a challenge to inorganic chemists, because the metastable cluster had been thought to exist only in a protein environment, and because chemical synthesis of the [8Fe-7S] core is inevitable to gain chemical insights into the biological function of the P-cluster. Molybdenum(vanadium)/iron/sulfur clusters having topological analogy with the P^N-cluster, $[(Tp)_2M_2Fe_6S_9(SH)_2]^{n-}$ ($n = 3$, 4; Tp = tris(pyrazolyl)borate), have been synthesized via core conversion of corresponding edge-bridged double cubane [2M-6Fe-9S] clusters.[7] These P^N-type clusters contain molybdenum or vanadium at both of the peripheral positions. On the other hand, we have employed a new approach to the construction of the inorganic [8Fe-7S] core of P-cluster in a nonpolar solvent, and have previously reported the synthesis of $[\{N(SiMe_3)_2\}\{SC(NMe_2)_2\}Fe_4S_3]_2(\mu_6\text{-}S)\{\mu\text{-}N(SiMe_3)_2\}_2$ (**1**)[8] via a reaction of an Fe(II) amide complex $Fe\{N(SiMe_3)_2\}_2$,[9] TipSH (Tip = 2,4,6-$^iPr_3C_6H_2$), thiourea ($SC(NMe_2)_2$), and elemental sulfur (S_8) in toluene. This method has been extended to the synthesis of another class of unprecedented [8Fe-7S] clusters, $[(DmpS)Fe_4S_3]_2(\mu\text{-}SDmp)_2(\mu\text{-}STip)(\mu_6\text{-}S)$ (Dmp = 2,6-(mesityl)$_2C_6H_3$) and $[(TipS)Fe_4S_3]_2(\mu\text{-}SDmp)_2\{\mu\text{-}N(SiMe_3)_2\}(\mu_6\text{-}S)$, which serve as topological links between the FeMo-cofactor, the FeFe-cofactor, and the P-cluster of nitrogenases.[10]

The model complex **1** reproduces the [8Fe-7S] core geometry of the P^N-cluster, while the 6Fe(II)−2Fe(III) oxidation states of **1** contrasts to the 8Fe(II) state of P^N. An obvious difference between **1** and the P^N-cluster is the ligand setting at iron atoms as drawn in Chart 1, where the inorganic core of P^N are bound to six cystein residues, while the inorganic core of **1** carries four amide and two thiourea ligands. In order to expand the scope of the model [8Fe-7S] clusters, and to gain deeper insights into the physicochemical properties of the P-cluster, we have synthesized a series of [8Fe-7S] clusters, in which the amide and thiourea ligands of **1** are substituted by thiolates. Development of a high yield synthesis of **1** was a key to the successful isolation of a variety of [8Fe-7S] clusters. This paper reports these model [8Fe-7S] clusters with new ligand settings, which resemble the native P-cluster more closely than **1**. Examination of their electrochemistry, Mössbauer spectra, and magnetic behaviors has allowed us to pursue the electronic properties and structure−function relationship of the native P-cluster.

2. Results and Discussion

2.1. Synthesis of the [8Fe-7S] Cluster 1. Complex **1** was synthesized from successive addition of toluene solutions of HSTip, tetramethylthiourea ($SC(NMe_2)_2$), and elemental sulfur (S_8) to a Schlenk tube containing $Fe\{N(SiMe_3)_2\}_2$ in the ratio 8(Fe):12(TipSH):3($SC(NMe_2)_2$):7(S) (Scheme 1). This optimized ratio of the reactants is rationalized as follows. Since the cluster **1** consists of 8 iron centers, 8 molecules of $Fe\{N(SiMe_3)_2\}_2$ are required, and thus 16 amide ligands are also present. The amide ligand is known to serve as a Brønsted base, and it can deprotonate a thiol to provide a metal−thiolate and an amine.[11] Thus, 12 protons, in this case from HSTip, are required to

Scheme 1

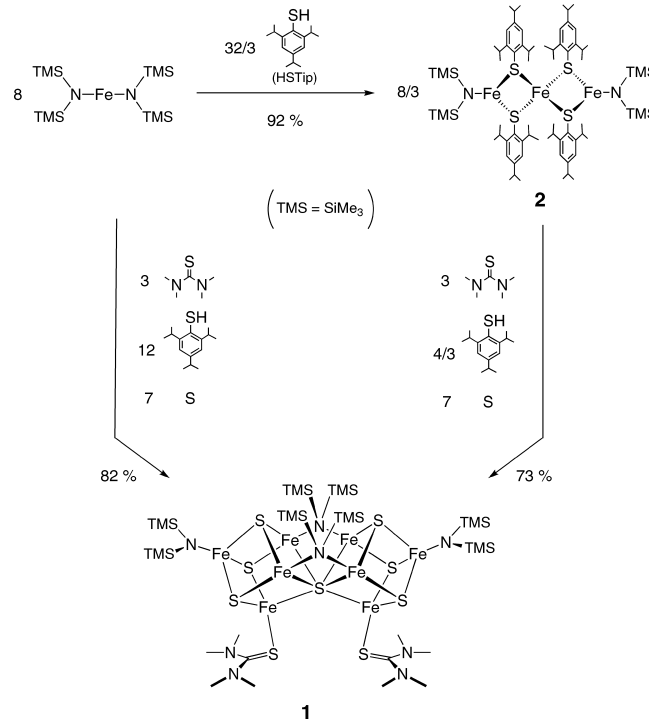

(4) (a) Lowe, D. J.; Fisher, K.; Thorneley, R. N. F. *Biochem. J.* **1993**, *292*, 93–98. (b) Peters, J. W.; Fisher, K.; Newton, W. E.; Dean, D. R. *J. Biol. Chem.* **1995**, *270*, 27007–27013. (c) Lanzilotta, W. N.; Seefeldt, L. C. *Biochemistry* **1996**, *35*, 16770–16776. (d) Chan, J. M.; Christiansen, J.; Dean, D. R.; Seefeldt, L. C. *Biochemistry* **1999**, *38*, 5779–5785.

(5) (a) McLean, P. A.; Papaefthymiou, V.; Orme-Johnson, W. H.; Münck, E. *J. Biol. Chem.* **1987**, *262*, 12900–12903. (b) Lindahl, P. A.; Papaefthymiou, V.; Orme-Johnson, W. H.; Münck, E. *J. Biol. Chem.* **1988**, *263*, 19412–19418. (c) Surerus, K. K.; Hendrich, M. P.; Christie, P. D.; Rottgardt, D.; Orme-Johnson, W. H.; Münck, E. *J. Am. Chem. Soc.* **1992**, *114*, 8579–8590.

(6) (a) Peters, J. W.; Stowell, M. H. B.; Soltis, S. M.; Finnegan, M. G.; Johnson, M. K.; Rees, D. C. *Biochemistry* **1997**, *36*, 1181–1187. (b) Mayer, S. M.; Lawson, D. M.; Gormal, C. A.; Roe, S. M.; Smith, B. E. *J. Mol. Biol.* **1999**, *292*, 871–891.

(7) (a) Zhang, Y.; Zuo, J.-L.; Zhou, H.-C.; Holm, R. H. *J. Am. Chem. Soc.* **2002**, *124*, 14292–14293. (b) Zhang, Y.; Holm, R. H. *J. Am. Chem. Soc.* **2003**, *125*, 3910–3920. (c) Zuo, J.-L.; Zhou, H.-C.; Holm, R. H. *Inorg. Chem.* **2003**, *42*, 4624–4631. (d) Zhang, Y.; Holm, R. H. *Inorg. Chem.* **2004**, *43*, 674–682. (e) Berlinguette, C. P.; Holm, R. H. *J. Am. Chem. Soc.* **2006**, *128*, 11993–12000. (f) Berlinguette, C. P.; Miyaji, T.; Zhang, Y.; Holm, R. H. *Inorg. Chem.* **2006**, *45*, 1997–2007.

(8) Ohki, Y.; Sunada, Y.; Honda, M.; Katada, M.; Tatsumi, K. *J. Am. Chem. Soc.* **2003**, *125*, 4052–4053.

(9) Andersen, R. A.; Faegri, K, Jr.; Green, J. C.; Haaland, A.; Lappert, M. F.; Leung, W.-P.; Rypdal, K. *Inorg. Chem.* **1988**, *27*, 1782–1786.

neutralize 12 amides, leaving 4 amides in the product. Interestingly, no thiolate was incorporated into the cluster **1**. The absence of thiolate ligands in **1** is probably due to reductive elimination of the disulfide TipS-STip, which can be produced upon oxidation of an intermediate iron-STip species by elemental sulfur. The number of sulfurs needed is 7, to produce the [8Fe-7S] core. The reduction of 7 S atoms to sulfide dianions requires 14 electrons, 12 of which come from formation of the TipS-STip disulfides, and 2 from iron atoms to produce two Fe(III) ions. The logical amount of $SC(NMe_2)_2$ needed for this cluster is 2, but 3 equiv were found to give a better yield. The yield of **1** as crystals from this reaction was reported earlier by us to be 28%.[8] We have found that the yield improves to 82% by slow crystallization and scaling up of the reaction, as described in the experimental section, so that further studies of the [8Fe-7S] cluster became feasible.

Alternatively, **1** was isolated in a good yield from the reaction of the preformed trinuclear thiolate/amide complex $Fe_3\{N(SiMe_3)_2\}_2(\mu\text{-STip})_4$ (**2**)[12] with HSTip, $SC(NMe_2)_2$, and S_8 in the ratio 8/3(**2**):4/3(HSTip):3($SC(NMe_2)_2$):7(S). This ratio also follows the same assumptions as described above. Gradual formation of cluster **1** occurred in 12 h at 30 °C, and standing the reaction mixture at ambient temperature for a week gave crystals of **1** in 73% yield. It is interesting to note that the yellowish dark brown color of **2** in toluene is very similar to that seen at the initial stage of the synthesis of **1** from the $Fe\{N(SiMe_3)_2\}_2$/TipSH/$SC(NMe_2)_2$/S_8 reaction system, i.e., when a toluene solution is added to $Fe\{N(SiMe_3)_2\}_2$. This color change indicates that **2** could be an intermediate in the pathway to **1**.

2.2. Ligand Substitution of Cluster 1. In order to replace the $N(SiMe_3)_2$ and/or $SC(NMe_2)_2$ ligands in **1** with thiolates, the two following approaches were investigated. One is addition of appropriate thiolate anions to **1** to substitute the thioureas, which are probably more labile than the $N(SiMe_3)_2$ ligands. The other is an acid−base reaction between the terminal $N(SiMe_3)_2$ ligands and thiols. The ligand substitution reactions based on these approaches have turned out not to be easy, because **1** is unstable toward nucleophiles such as thiolates in polar solvents, and toward protic substances such as thiols, causing degradation into thermodynamically more stable [4Fe-4S] clusters (vide infra).

2.2.1. Replacement of $SC(NMe_2)_2$ Ligands. In initial attempts to substitute the $SC(NMe_2)_2$ ligands with thiolates, reactions of cluster **1** with 2 equiv of tetraethylammonium salts of various para(ortho)-substituted-aryl-thiolates were examined in THF at −40 °C. The reactions with aryl-thiolates apparently occurred, and the expected bis(thiolato)-[8Fe-7S] cluster dianions were detected as major products in electro-spray ionization mass spectra (ESI-MS) of the reaction mixtures. However, attempts at crystallization resulted in the formation of a black oily material. Unsuccessful isolation of the product was attributed to the formation of byproducts associated with degradation of

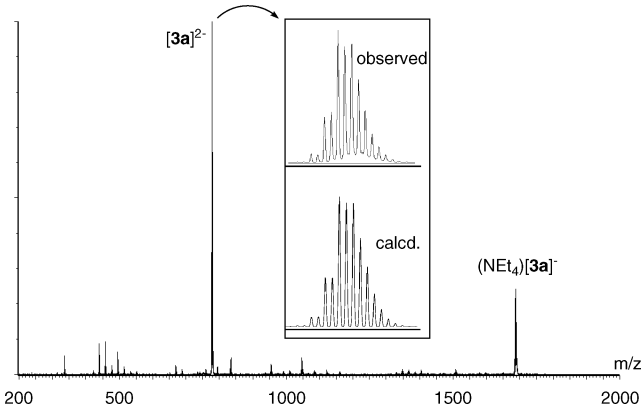

Figure 1. Electrospray ionization mass spectrum (ESI-MS) of the reaction mixture of **1** and $(NEt_4)(SC_6H_4\text{-}4\text{-}Me)$ in fluorobenzene/THF.

Scheme 2

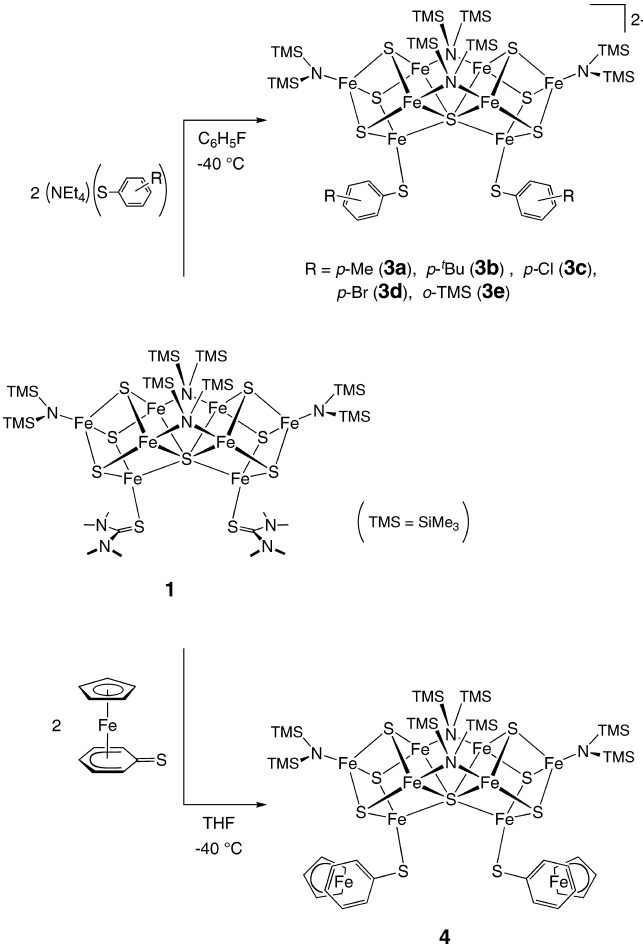

[8Fe-7S] clusters into [4Fe-4S] clusters, which were seen in the ESI-MS spectra at about 30% of the intensity of the desired bis(thiolato)-[8Fe-7S] clusters. Decomposition of the [8Fe-7S] core to [4Fe-4S] clusters appears to be facilitated by thiolate anions in THF solutions. The ESI-MS measurements indicated that addition of excess tetraethylammonium thiolates to a THF solution of **1** resulted in the dominant formation of [4Fe-4S] clusters.

Therefore we sought suitable reaction conditions to prevent the formation of [4Fe-4S] byproducts. In order to decrease the amount of free thiolate anion in solution, we sought a less polar solvent to which the ionic thiolate was less soluble. Fluoroben-

(10) Ohki, Y.; Ikagawa, Y.; Tatsumi, K. *J. Am. Chem. Soc.* **2007**, *129*, 10457–10465.
(11) (a) Ellison, J. J.; Ruhlandt-Senge, K.; Power, P. P. *Angew. Chem., Int. Ed. Engl.* **1994**, *33*, 1178–1180. (b) Hauptmann, R.; Klib, R.; Schneider, J.; Henkel, G. *Z. Anorg. Allg. Chem.* **1998**, *624*, 1927–1936. (c) Komuro, T.; Kawaguchi, H.; Tatsumi, K. *Inorg. Chem.* **2002**, *41*, 5083–8090. (d) Ohta, S.; Ohki, Y.; Ikagawa, Y.; Suizu, R.; Tatsumi, K. *J. Organomet. Chem.* **2007**, *692*, 4792–4799. (e) Pryadun, R.; Holm, R. H. *Inorg. Chem.* **2008**, *47*, 3366–3370.
(12) MacDonnell, F. M.; Ruhlandt-Senge, K.; Ellison, J. J.; Holm, R. H.; Power, P. P. *Inorg. Chem.* **1995**, *34*, 1815–1822.

Scheme 3. Degradation of the [8Fe-7S] Core in the Presence of Thiols

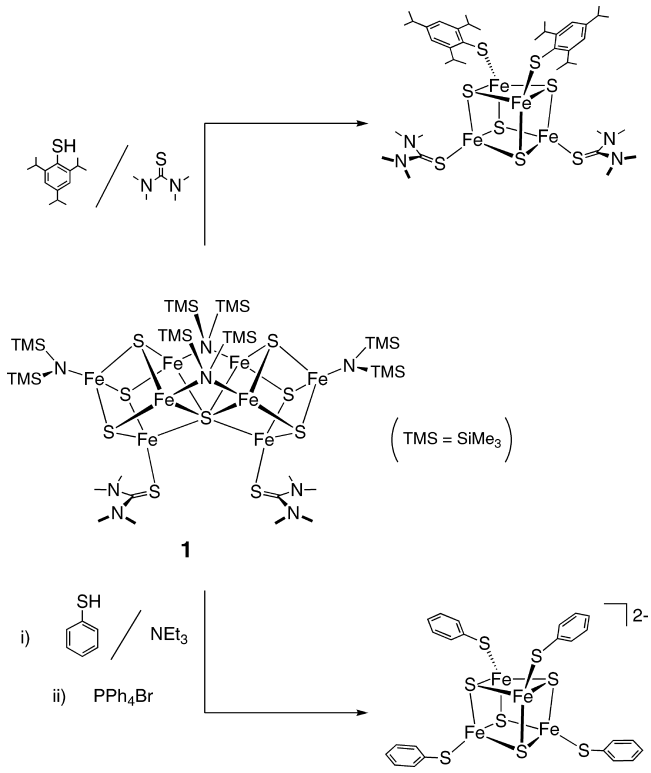

zene proved to be an appropriate media, as it is less polar than THF but still retains some ability to dissolve thiolate salts. Treatment of **1** with 2 equiv of $(NEt_4)(SC_6H_4$-p-$CH_3)$ in fluorobenzene at −40 °C gave initially a suspension, which gradually became a dark brown solution over a few hours. The expected bis(thiolato)-[8Fe-7S] cluster $[[\{N(SiMe_3)_2\}(SC_6H_4$-$p$-$CH_3)_2Fe_4S_3]_2(\mu_6$-S$)\{\mu$-$N(SiMe_3)_2\}_2]^{2-}$ (**3a**) was observed as the dominant product in the ESI-MS spectrum, as shown in Figure 1. Clean conversion from **1** to **3a** also facilitated successful crystallization from THF, and the analytically pure product of **3a** was isolated in 24% yield. In a similar manner, a series of bis(thiolato)-[8Fe-7S] clusters $[[\{N(SiMe_3)_2\}(SC_6H_4$-$R)_2Fe_4S_3]_2(\mu_6$-S$)\{\mu$-$N(SiMe_3)_2\}_2]^{2-}$ (R = p-^{t}Bu, **3c**; R = p-Cl, **3d**; R = p-Br, **3e**; R = o-$SiMe_3$) were obtained as crystals in 23−65% yields (Scheme 2, top).

We also became interested in the η-cyclohexadienethionyl/η-cyclopentadienyl sandwich complex of iron, $CpFe(C_6H_5S)$,[13] because it may serve as a zwitterionic thiolate ligand where the anionic center resides at the sulfur atom with the cationic center at iron. Replacement of the $SC(NMe_2)_2$ ligands in **1** with $CpFe(C_6H_5S)$ allows the introduction of two thiolate ligands into the [8Fe-7S] core of **1**, while leaving the cluster uncharged. The resulting bis(thiolato)-[8Fe-7S] cluster is anticipated to facilitate isolation of neutral tetrakis(thiolate)-[8Fe-7S] clusters by replacement of the terminal amides with thiolates, as will be described later in this paper. The reaction of **1** with 2 equiv of $CpFe(C_6H_5S)$ proceeded smoothly even in THF at −40 °C, and the neutral bis(thiolato)-[8Fe-7S] cluster $[\{N(SiMe_3)_2\}\{CpFe(C_6H_5S)\}Fe_4S_3]_2(\mu_6$-S$)\{\mu$-$N(SiMe_3)_2\}_2$ (**4**) was isolated as a black crystalline solid in 74% yield (Scheme 2, bottom). It should be noted here that $CpFe(C_6H_5S)$ is moderately light sensitive. Thus, the synthesis of **4** and the crystallization from THF/toluene were carried out by shielding the reaction solutions from the light.

Scheme 4

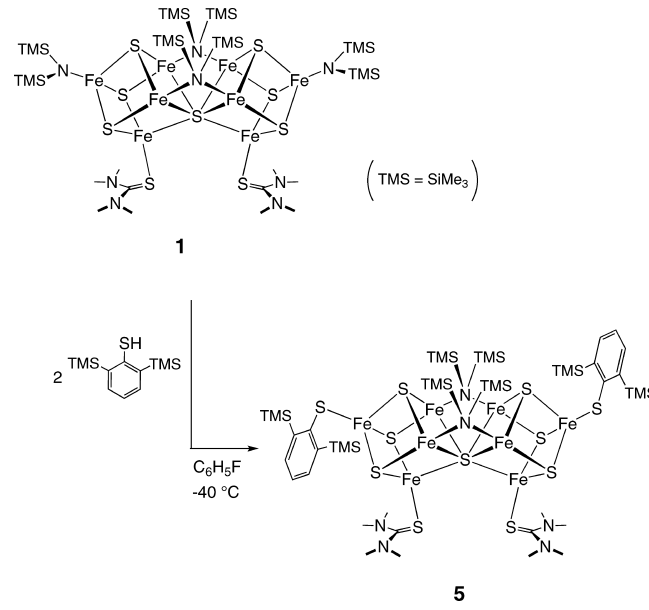

2.2.2. Replacement of the Terminal $N(SiMe_3)_2$ Ligands. In an attempt to substitute the amide ligands, we first examined the reaction of **1** with 4 equiv of HSTip in toluene, to find that apparent decomposition/fragmentation of the [8Fe-7S] core occurs. Although characterization of the decomposed product(s) was not possible from this reaction, addition of $SC(NMe_2)_2$ to the **1**/ HSTip reaction mixture allowed us to isolate the neutral cubane cluster $Fe_4S_4(STip)_2\{SC(NMe_2)_2\}_2$[14] in 38% yield as crystals (Scheme 3). The reaction of **1** with PhSH in acetonitrile in the presence of NEt_3 also induced fragmentation of the [8Fe-7S] core, and the subsequent cation exchange with PPh_4Br led to isolation of the cubane cluster dianion $(PPh_4)_2[Fe_4S_4(SPh)_4]$[15] in 43% yield.

It is conceivable that the degradation of the [8Fe-7S] core of **1** is triggered by the cleavage of the Fe−(μ-amide)-Fe bonds upon protonation of the μ-amide ligands by thiols. We hypothesized that bulky thiols might substitute the terminal amides selectively leaving the μ-amides intact, because the amide nitrogen atoms on the peripheral iron atoms are less sterically hindered. Thus, HSBtp (Btp = 2,6-$(SiMe_3)_2C_6H_3$)[16] was treated with **1** at −40 °C in fluorobenzene, and the bis-thiolate cluster $[(SBtp)\{SC(NMe_2)_2\}Fe_4S_3]_2(\mu_6$-S$)\{\mu$-$N(SiMe_3)_2\}_2$ (**5**) was in fact isolated in 21% yield upon crystallization of the crude product from toluene/hexane (Scheme 4). Although the isolated yield of crystalline **5** was not very high, which is in part due to its high solubility in toluene, generation of [4Fe-4S] clusters was not discernible in this reaction. It appears that the $SiMe_3$ groups at the ortho positions in HSBtp protect the SH moiety sufficiently to hinder the reaction with the μ-amides to take place.

2.2.3. Synthesis of Tris(thiolate)- and Tetrakis(thiolate)-[8Fe-7S] Clusters. We next combined the two approaches of ligand

(13) Helling, J. F.; Hendrickson, W. A. *J. Organomet. Chem.* **1979**, *168*, 87–95.
(14) Bierbach, U.; Saak, W.; Haase, D.; Pohl, S. *Z. Naturforsch., B: Chem. Sci.* **1991**, *46*, 1629–1634.
(15) (a) Averill, B. A.; Herskovitz, T.; Holm, R. H.; Ibers, J. A. *J. Am. Chem. Soc.* **1973**, *95*, 3523–3534. (b) Gloux, J.; Gloux, P.; Hendriks, H.; Rius, G. *J. Am. Chem. Soc.* **1987**, *109*, 3220–3224.
(16) Block, E.; Eswarakrishnan, V.; Gernon, M.; Ofori-Okai, G.; Saha, C.; Tang, K.; Zubieta, J. *J. Am. Chem. Soc.* **1989**, *111*, 658–665.

Scheme 5

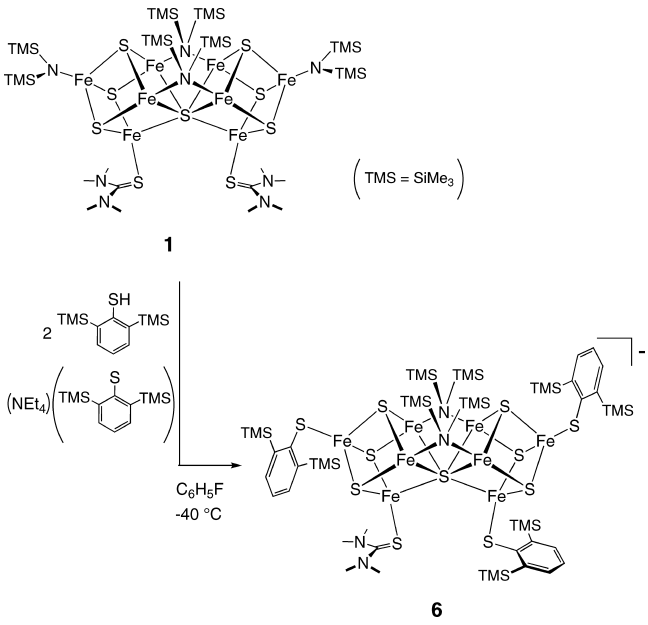

Scheme 6

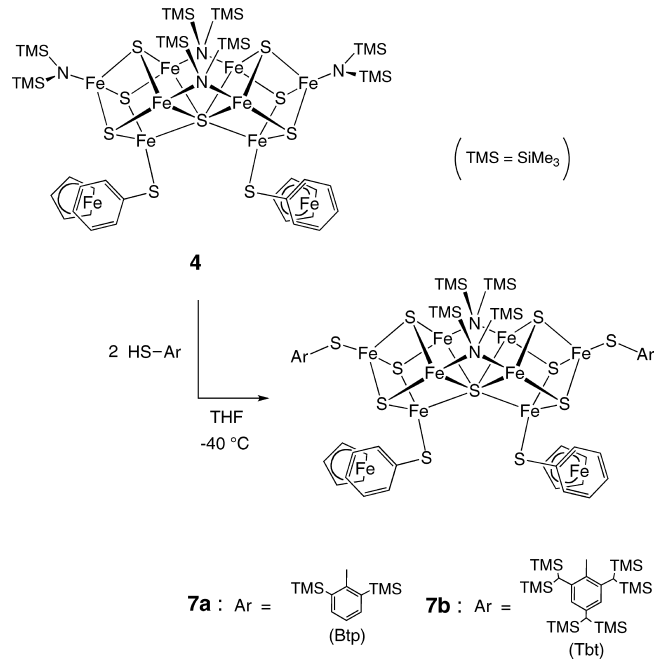

substitution reactions demonstrated in Schemes 2 and 4, in order to introduce more thiolate ligands to the [8Fe-7S] core. Treatment of **1** with 2 equiv of HSBtp in fluorobenzene at −40 °C was followed by addition of 2 equiv of $(NEt_4)(SC_6H_4$-4-Br), and the ESI-MS spectra of the reaction mixture showed an intense signal for the tetrakis(thiolato)-[8Fe-7S] cluster $[[(SBtp)(SC_6H_4$-4-Br$)Fe_4S_3]_2(\mu_6$-S$)\{\mu$-N$(SiMe_3)_2\}_2]^{2-}$ at m/z = 892.7. However this cluster was too unstable to isolate. On the other hand, a small amount of crystalline tris(thiolate)-[8Fe-7S] cluster $[[(SBtp)\{SC(NMe_2)_2\}Fe_4S_3][(SBtp)_2Fe_4S_3](\mu_6$-S$)\{\mu$-N$(SiMe_3)_2\}_2]^-$ (**6**) was isolated from the reaction of **1** with 2 equiv of HSBtp and 1 equiv of (NEt_4)(SBtp) at −40 °C (Scheme 5). Substitution of the remaining $SC(NMe_2)_2$ ligand in **6** with SBtp was not successful, perhaps because the steric bulk of the Btp substituent does not allow the cluster to accommodate four SBtp lignds.

Introduction of four thiolate ligands onto the [8Fe-7S] core was finally achieved by choosing the noncharged bis(thiolate)-[8Fe-7S] cluster **4** as a target for thiolate substitution of the terminal amides. As is described earlier in this paper, bulky thiols are required for selective substitution at the terminal amides. Therefore, **4** was treated with 2 equiv of HSBtp or HSTbt (Tbt = 2,4,6-$\{(SiMe_3)_2CH\}_3C_6H_2$)[17] in THF at −40 °C. The reaction solutions were shielded from the light, considering the light sensitive nature of CpFe(η^6-C_6H_5S). From these reactions, tetrakis(thiolate)-[8Fe-7S] clusters $[(SAr)\{CpFe(\eta^6$-$C_6H_5S)\}Fe_4S_3]_2(\mu_6$-S$)\{\mu$-N$(SiMe_3)_2\}_2$ (**7a**; Ar = Btp, **7b**; Ar = Tbt) were isolated as anallitically pure crystalline solids in moderate yields (Scheme 6). Crystals suitable for the X-ray analysis were obtained for **7b** from a THF/cyclohexane solution.

2.2.4. Instability of the [8Fe-7S] Core. The P-cluster model complexes are not stable toward both thiolate anions and thiols. The degradation of [8Fe-7S] core of **1** into [4Fe-4S] cubane clusters, which occurs in the reactions with thiolate anions in THF, is probably triggered by the nucleophilic attack of thiolates at iron centers. The polar solvent appears to facilitate this nucleophlic attack due to the higher solution concentration of thiolate salts in THF compared to less polar solvents, e.g., fluorobenzene. A polar solvent itself may also act as a nucleophile and promotes the ligand exchange. For instance, *N*-methyl formamide (NMF) was reported to replace the αCys-275 and αHis-442 residues bound to the FeMo-cofactor of *A. vinelandii*.[18] It is also known that intermolecular thiolate/chloride ligand exchange between $[Fe_4S_4Cl_4]^{2-}$ and $[Fe_4S_4(SPh)_4]^{2-}$ occurs in dimethylformamide (DMF) generating $[Fe_4S_4Cl_2(SPh)_2]^{2-}$.[19] For the synthesis of **1**, **3a**−**e**, and **4**, the use of polar solvents should be avoided to retain the metastable [8Fe-7S] core. The structural similarity between **1** and the native P^N-cluster raises the possibility that non-nucleophilic protein environment is crucial for the biosynthesis and kinetic stabilization of the P-cluster. In fact, the native P-cluster resides in a hydrophobic pocket of less nucleophilic residues such as βTyr-98, αTyr-91, αTyr-64, and βPhe-99 at the interface of the αβ-subunits.[6]

On the other hand, vulnerability of the [8Fe-7S] core of **1** toward thiols resembles the instability of the native P-cluster toward the dithiol-promoted extrusion of the cluster core from the MoFe-proteins. Attempts to extrude the P-cluster of *Clostridium pasteurianum* and *A. vinelandii* with dithiols resulted in degradation of the cluster core, and 90−103% of the Fe content was isolated as $[Fe_4S_4(SR^F)_4]^{2-}$, after the subsequent ligand exchange of the initial extrusion products with HS-*p*-$CF_3C_6H_4$ (HSR^F).[20] The Mo/Fe/S cluster, $[(Tp)_2Mo_2Fe_6S_9(SH)_2]^{3-}$, which is structurally relevant to **1** and the P-cluster, was also reported to split into two $[MoFe_3S_4]$ cubane clusters when treated with $(Et_3NH)(BPh_4)$ or HS-*p*-tol.[7b]

2.3. Structures of the [8Fe-7S] Clusters. The structures of **1**, **3a**−**3e**, **4**−**6**, and **7b** have been determined by X-ray crystal-

(17) Takeda, N.; Shimizu, D.; Tokitoh, N. *Inorg. Chem.* **2005**, *44*, 8561–8568.

(18) (a) Shah, V. K.; Brill, W. J. *Proc. Natl. Acad. Sci. U.S.A.* **1977**, *74*, 3249–3253. (b) McLean, P. A.; Wink, D. A.; Chapman, S. K.; Hickman, A. B.; McKillop, D. M.; Orme-Johnson, W. H. *Biochemistry* **1989**, *28*, 9402–9406. (c) Ma, L.; Gavini, N.; Liu, H. I.; Hedman, B.; Hodgson, K. O.; Burgess, B. K. *J. Biol. Chem.* **1994**, *269*, 18007–18015.

(19) Coucouvanis, D.; Kanatzidis, M.; Simhon, E.; Baenziger, N. C. *J. Am. Chem. Soc.* **1982**, *104*, 1874–1882.

(20) Kurts, D. M., Jr.; McMillan, R. S.; Burgess, B. K.; Mortenson, L. E.; Holm, R. H. *Proc. Natl. Acad. Sci. U.S.A.* **1979**, *76*, 4986–4989.

Table 1. Selected Distances (Å) and Angles (deg) for Clusters **1**, **3a**−**3e**, **4**−**6**, and **7b**[a]

cluster	Fe1−Fe2, Fe1−Fe3, Fe1−Fe4 Fe5−Fe6, Fe5−Fe7, Fe5−Fe8	Fe2−Fe3, Fe2−Fe4, Fe3−Fe4 Fe6−Fe7, Fe6−Fe8, Fe7−Fe8	Fe2−Fe7, Fe3−Fe6
1	2.8275(6), 2.8147(6), 2.7346(6)	2.7021(7), 2.6505(7), 2.6429(7)	2.7910(5)
3a	2.7951(16), 2.793(2), 2.7763(16) 2.8013(16), 2.743(2), 2.7646(19)	2.704(2), 2.6338(16), 2.631(2) 2.688(2), 2.6449(17), 2.628(2)	2.743(2), 2.723(2)
3b	2.8019(12), 2.8080(12), 2.7698(12)	2.6897(17), 2.6580(12), 2.6657(13)	2.7270(12)
3c	2.814(3), 2.806(2), 2.772(5) 2.799(12), 2.803(2), 2.786(4)	2.697(10), 2.630(8), 2.642(3) 2.709(11), 2.635(8), 2.635(2)	2.736(8), 2.721(8)
3d	2.7965(12), 2.8150(12), 2.7611(12) 2.8000(12), 2.8350(12), 2.7510(12)	2.7294(11), 2.6107(11), 2.6188(11) 2.7146(11), 2.6243(11), 2.6198(11)	2.7383(11), 2.7238(11)
3e	2.7991(12), 2.8120(12), 2.7836(11)	2.7031(12), 2.6389(12), 2.6326(12)	2.7108(12)
4	2.8066(6), 2.8220(6), 2.7567(6) 2.8260(6), 2.8500(6), 2.7787(7)	2.7098(6), 2.6508(6), 2.6312(6) 2.7284(6), 2.6145(7), 2.6095(7)	2.7502(6), 2.7529(6)
5	2.7851(6), 2.7962(5), 2.7138(6) 2.7399(5), 2.7734(5), 2.6990(6)	2.7250(5), 2.6787(6), 2.6430(5) 2.7393(5), 2.6581(5), 2.6065(5)	2.7627(5), 2.7405(5)
6	2.7518(19), 2.7551(18), 2.786(2) 2.7767(19), 2.7645(18), 2.7148(18)	2.7691(13), 2.7504(17), 2.7358(17) 2.7037(13), 2.6156(19), 2.6141(19)	2.703(2), 2.723(2)
7b	2.7215(15), 2.7662(17), 2.7139(16) 2.7175(14), 2.7594(15), 2.7093(16)	2.7348(14), 2.6238(15), 2.6390(17) 2.7333(14), 2.6224(13), 2.6583(15)	2.7204(15), 2.7017(14)

[a]Labeling scheme as shown. $N = N(SiMe_3)_2$.

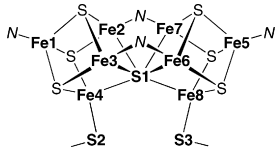

cluster	Fe4−S1, Fe8−S1	Fe4−S1−Fe8	Fe4−S2, Fe8−S3
1	2.3492(5)	143.61(6)	2.3151(10)
3a	2.404(2), 2.405(2)	151.01(9)	2.275(2), 2.280(2)
3b	2.3949(9)	149.60(9)	2.3105(17)
3c	2.395(7)	151.28(8)	2.285(2), 2.276(2)
3d	2.4112(17), 2.3980(17)	151.66(6)	2.2573(17), 2.264(2)
3e	2.4174(9)	153.43(9)	2.292(2)
4	2.3847(9), 2.4030(8)	149.36(4)	2.2925(11), 2.3056(12)
5	2.3509(8), 2.3974(8)	146.79(3)	2.3340(9), 2.3067(10)
6	2.430(2), 2.384(2)	148.48(11)	2.312(3), 2.325(3)
7b	2.406(2), 2.406(2)	150.92(9)	2.321(2), 2.314(2)

lography, and their selected bond distances and angles are summarized in Table 1, while the ORTEP drawings are shown in Figure 2 for **1**, **3a**, **4**, **5**, and **7b**. The [8Fe-7S] cluster cores consist of two [4Fe-3S] incomplete cubanes, which are connected by a μ_6-sulfur atom denoted S1 in Table 1. Two μ-amide ligands further link the cuboidal units, each bridging two Fe atoms, and this corner-shared double cubane structure is bent at S1 toward the side where the μ-amides are situated. Consequently, the Fe4−(μ_6-S)−Fe8 angles are large, ranging from 143.61(6)° of **1** to 153.43(9)° of **3e**. For all the [8Fe-7S] clusters, the Fe−Fe distances within each [4Fe-3S] unit can be classified into two groups. The Fe−Fe distances associated with the peripheral iron atoms (Fe1/Fe5) are long, the averages being 2.7313(16)−2.8067(7) Å, as compared with those of other Fe−Fe distances of 2.6529(11)−2.6981(17) Å. This may be partly due to coordination of amide, a strong-donor ligand, at Fe1 and Fe5. The Fe−(μ_6-S) distances are understandably longer (2.3489(5)−2.4373(14) Å) than the Fe−(μ_3-S) distances (2.223(2)−2.3093(11) Å).

Substitution of $SC(NMe_2)_2$ in **1** with thiolates leads to elongation of the Fe4/Fe8-(μ_6-S) bonds from 2.3492(5) Å (**1**) to 2.3847(9)−2.4174(9) Å (**3a**−**3e** and **4**). The Fe−S bonding with the μ_6-sulfur is relatively weak and the bond lengths are sensitive to the electronic property of the iron atoms. The thiolates are better donor than thiourea, and stronger trans influence may be a reason for elongation of the Fe−(μ_6-S) bonds in **3a**−**3e** and **4**. The substitution also causes opening of the Fe4−(μ_6-S)−Fe8 bond angle from 143.61(6)° (**1**) to 149.36(4)−153.43(9)° (**3a**−**3e** and **4**), which in turn results in shortening of the Fe2−Fe7 and Fe3−Fe6 distances by 0.04−0.08 Å. The X-ray structure of **4** needs further comments on the coordination of $CpFe(C_6H_5S)$. The C_6H_5S group of $CpFe(C_6H_5S)$ can be seen either as a benzenethiolate ($^-S-C_6H_5$) or as a cyclohexadienethionyl ($S{=}C_6H_5^-$) moiety. The Fe−C_{ipso} bond lengths in **4** (2.165(4), 2.179(4) Å) are longer, but only slightly by 0.07−0.11 Å, than the other Fe−C(C_6H_5S) lengths, while the S−C bond distances of the C_6H_5S groups in **4** (1.728(3), 1.729(4) Å) are substantially longer than the S=C distance of thioketones (1.61−1.67 Å).[21] These geometric features point to a benzenethiolate character of the $CpFe(C_6H_5S)$ ligand, and thus the ligand is zwitterionic with an anionic center residing at the sulfur atom and a cationic center at the iron atom.[22]

2.4. Structural Relevance to the Native P-Cluster. Two forms of the P-cluster, designated as the P^N and P^{OX} (or P^{2+}) states, have been crystallographically identified,[6] and the P^N and P^{OX} clusters have been suggested to consist of 8Fe(II) and 6Fe(II)−2Fe(III) centers, respectively.[5] The X-ray structures of their [8Fe-7S] inorganic cores are compared with that of **1** in Figure 3. It is evident that the cluster structure of **1** reproduces very well that of the P^N-cluster, whereas their electron counts are different by two electrons. On the other hand, the [8Fe-7S] structure reported for the P^{OX} cluster differs significantly from those of **1** and P^N, while the 6Fe(II)−2Fe(III) oxidation state of P^{OX} is the same as that of **1**. In the crystal structure of the

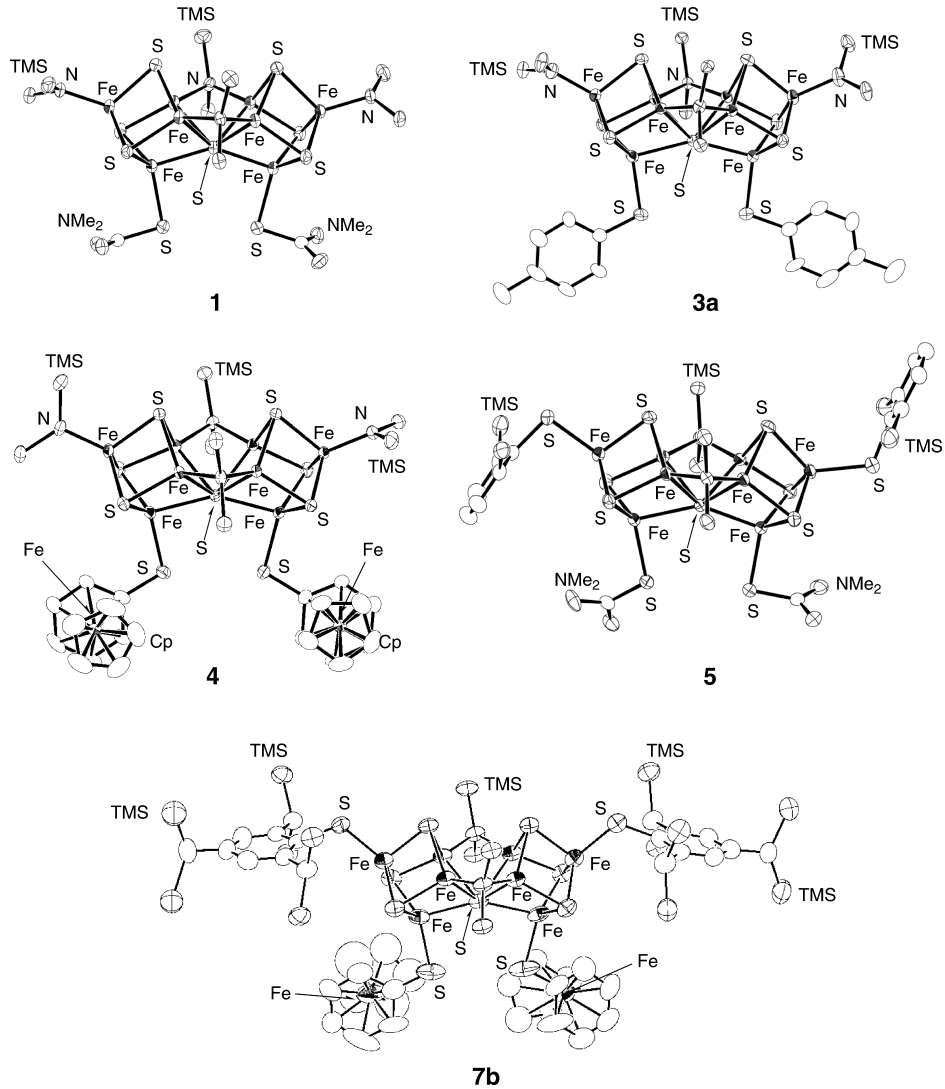

Figure 2. Perspective views of **1**, **3a**, **4**, **5**, and **7b**. The methyl groups of $SiMe_3$ (TMS) and $SC(NMe_2)_2$ are omitted for clarity. One of the Cp groups and two $SiMe_3$ groups in **7b** are disordered over two positions, and one of each is shown for clarity.

P^{OX} state of *A. vinelandii*, two protein residues are bound to the iron centers of the cluster core, in addition to a set of cysteine residues. These are an amide nitrogen of αCys-88 and an oxygen atom of *β*Ser-188, which pull two of the six inner iron atoms away from the central sulfur atom. As a result, the central sulfur atom becomes four-coordinate, bonding to three iron atoms from one of the cuboidal [4Fe-3S] units and one iron atom from the other.

Although we do not have a clear explanation for the distorted structure of the P^{OX}, the structural similarity between the P^N cluster and our model clusters, **1** and its variants (**3a**−**e**, **4**−**6**, and **7b**), indicate that an [8Fe-7S] cluster with 6Fe(II) and 2Fe(III) can retain a structure quite like that of the P^N cluster. The quasi-reversible redox couples observed for the model [8Fe-7S] clusters (vide infra) also support this possibility. A common feature of redox-active [4Fe-4S], [3Fe-4S], and [2Fe-2S] clusters is that the core geometries do not change dramatically during their redox events. The structural rigidity is important for the effectiveness of iron−sulfur clusters in the electron-transfer reactions in nature, since the substantial structural change would obstruct the reversibility of their redox processes. Therefore, it might be that the intriguing structure determined for P^{OX} does not really represent the P^{OX} state occurring in electron transfer processes of nitrogenase but could rather be another oxidized form generated by oxidation coupled to some chemical reaction or could be a degraded form, because preservation of redox states during crystallization and X-ray data collection can be challenging.[23]

2.5. Electrochemistry of [8Fe-7S] Clusters. The iron−sulfur proteins involved in electron-transfer processes, containing [4Fe-4S], [3Fe-4S], or [2Fe-2S] clusters, usually exhibit one-electron transfer.[24] On the other hand, the P-cluster has been suggested to carry out a reversible multielectron redox process, because

(21) For example: (a) Arjunan, P.; Ramamurthy, V.; Venkatesan, K. *Acta Crystallogr., Sect. C* **1984**, *40*, 552–555. (b) Tokitoh, N.; Choi, N.; Goto, N.; Ando, W. *J. Org. Chem.* **1989**, *54*, 4660–4663. (c) Tokitoh, N.; Noguchi, M.; Kabe, Y.; Ando, W.; Goto, M.; Maki, H. *Tetrahedron Lett.* **1990**, *31*, 7641–7644. (d) Bryce, M. R.; Coffin, M. A.; Hursthouse, M. B.; Mazid, M. *Angew. Chem., Int. Ed. Engl.* **1991**, *30*, 871–873. (e) Schroth, W.; Hintzsche, E.; Spitzner, R.; Irngartinger, H.; Siemund, V. *Tetrahedron Lett.* **1994**, *35*, 1973–1976. (f) Schroth, W.; Hintzsche, E.; Spitzner, R.; Strohl, D.; Sieler, J. *Tetrahedron* **1995**, *51*, 13247–13260. (g) Fu, T. Y.; Scheffer, J. R.; Trotter, J. *Acta Crystallogr., Sect. C* **1998**, *54*, 496–497. (h) Gleiter, R.; Gaa, B.; Sigwart, C.; Lange, H.; Borzyk, O.; Rominger, F.; Irngartinger, H.; Oeser, T. *Eur. J. Org. Chem.* **1998**, 171–176. (i) Shimada, K.; Nanae, T.; Aoyagi, S.; Takikawa, Y.; Kabuto, C. *Tetrahedron Lett.* **2001**, *42*, 6167–6169. (j) Selivanova, S. V.; Dolphin, D.; van Lier, J. E.; Kudrevich, S. V. *Inorg. Chim. Acta* **2003**, *349*, 58–64.

(22) For the analogous cluster **7b**, low quality of the X-ray data hampers us from discussing properties of the $CpFe(C_6H_5S)$ ligands in the cluster.

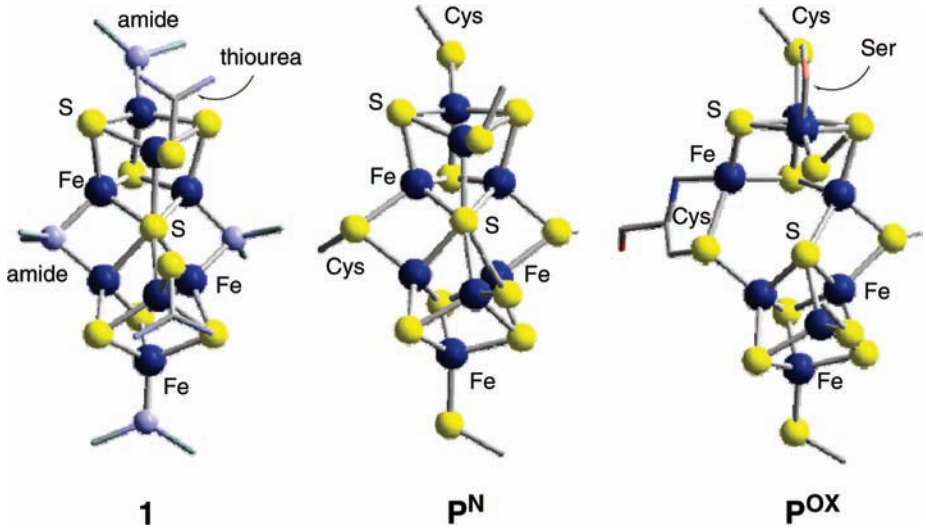

Figure 3. The [8Fe-7S] core structures of **1**, P^N, and P^{OX}. The methyl groups of $SiMe_3$ and $SC(NMe_2)_2$ in **1** are omitted for clarity. The coordinates of P^N and P^{OX} have been taken from the crystal data for the MoFe-proteins of *K. pneumoniae* nitrogenase, where the PDB codes are 1QGU and 1QH8, respectively.[6b]

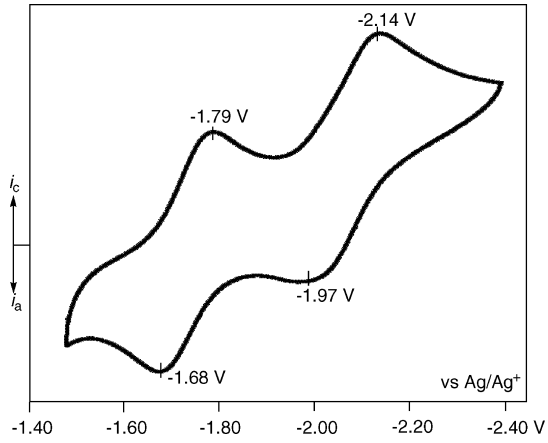

Figure 4. Cyclic voltammogram of **3a** in THF at room temperature.

the P-cluster exhibits multiple oxidation states, and in view of the fact that nitrogenase requires eight electrons to reduce molecular nitrogen into ammonia.[3,4] However, electronic properties of P-cluster has not been well understood, partly because appropriate model clusters were lacking. We therefore examined cyclic voltammograms of the model [8Fe-7S] clusters, and found that they all exhibit two quasi-reversible one-electron redox processes. Figure 4 shows the spectrum of **3a** measured in THF, and the $E_{1/2}$ values of **1**, **3a**−**e**, **5**, and **7a**,**b** are summarized in Table 2. The 6Fe(II)−2Fe(III) oxidation state of the model clusters corresponds to that of P^{OX}, while a two-electron reduction leads to the 8Fe(II) state of P^N. Thus, these models clearly demonstrate reversible redox between the two major oxidation states of the P-cluster. The two-electron redox process is probably accounted for the unique [8Fe-7S] core of P-cluster, which derives from two of the one-electron redox cubanes. The two redox potentials ($E_{1/2}$) for the $[A]/[A]^-$ and $[A]^-/[A]^{2-}$ couples are well separated, and therefore, an intermediary P^{1+} state could be isolated. Although we were unable to isolate the reduced product of **1**, we found an interesting C−H bond activation of decamethylcobaltocene mediated by **1**.[25]

Table 2. Redox Potentials for Clusters **1**, **3a**−**3e**, **5**, **7a**, and **7b**[a]

cluster [A]	$E_{1/2}$ for $[A]/[A]^-$ (V)	$E_{1/2}$ for $[A]^-/[A]^{2-}$ (V)
1	−1.29	−1.69
3a	−1.74	−2.06
3b	−1.89	−2.19
3c	−1.77	−2.11
3d	−1.90	−2.25
3e	−1.81	−2.15
5	−1.18	−1.51
7a	−1.26	−1.57
7b	−1.33	−1.68

[a] Potentials vs Ag/Ag^+ in THF.

Table 2 shows that the change of redox potential ($E_{1/2}$) for the $[A]/[A]^-$ couple parallels that for the $[A]^-/[A]^{2-}$ couple. These potential changes upon ligand substitution of **1** can partly be rationalized. For instance, replacement of the neutral thiourea ligands of **1** with thiolate anions to give **3a**−**3e** results in the notable negative shifts, simply because the negative charge of clusters makes reduction more difficult. On the other hand, substitution of the terminal amide ligands with thiolates, in going from **1** to **5**, leads to a slight positive shift, which could be attributed to the strong σ-/π-donation of amide ligands. This strong amide donation should be a reason why our model [8Fe-7S] clusters assume the 6Fe(II)−2Fe(III) state, which is two-electrons less than the 8Fe(II) state of P^N-cluster.

2.6. Mössbauer Spectra and Magnetic Properties of [8Fe-7S] Clusters. The model clusters have a 6Fe(II)−2Fe(III) mixed-valence state, and they were subjected to the Mössbauer study in order to examine the oxidation states of the iron centers in detail. The ^{57}Fe Mössbauer spectra of **1**, **3a**, and **5** were measured at 77 K (Figure 5). The isomer shifts (IS) and quadrupole splittings (QS) are summarized in Table 3, and they are compared with those for the native P^N-cluster.[5] The Mössbauer spectra of these model clusters each consists of two doublets with an intensity ratio of ca. 1:3. The weaker doublets appearing at IS = 0.37−0.38 mm/s can be assigned to those

(23) Rees, D. C.; Howard, J. B. *Curr. Opin. Chem. Biol.* **2000**, *4*, 559–566.
(24) Rao, P. V.; Holm, R. H. *Chem. Rev.* **2004**, *104*, 527–559.
(25) Ohki, Y.; Murata, A.; Imada, M.; Tatsumi, K. *Inorg. Chem.* **2009**, *48*, 4271–4273.

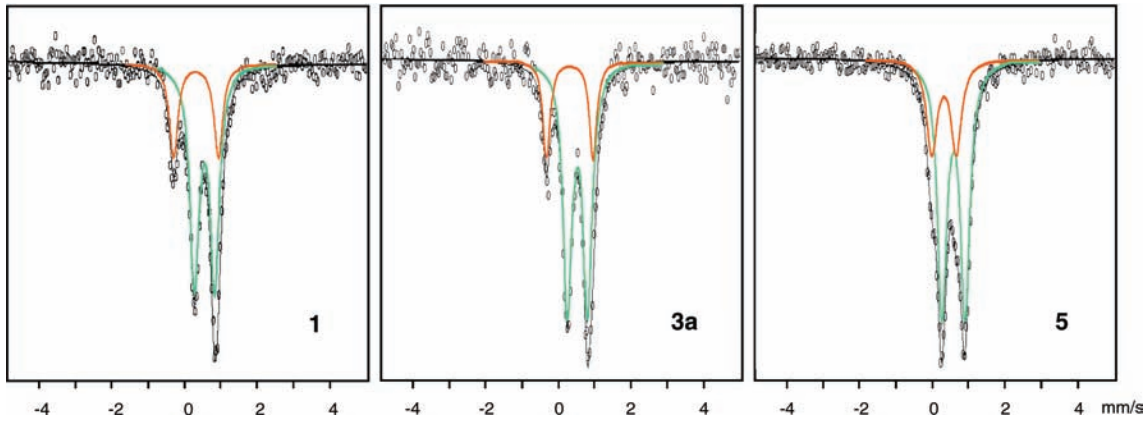

Figure 5. Mössbauer spectra of **1**, **3a**, and **5** at 77 K.

Table 3. ^{57}Fe Mössbauer Parameters for **1**, **3a**, **5**, and P^N-Cluster[a]

cluster	*T* (K)	isomer shift (mm/s)	quadrupole splitting (mm/s)	%
1	77	0.61	0.54	73
		0.37	1.28	27
3a	77	0.60	0.56	75
		0.38	1.30	25
5	77	0.64	0.64	74
		0.37	0.68	26
P^N-cluster[a]	4.2	0.61	1.34	75
		0.65	3.00	25

[a] Reference 5.

arising from Fe(III) sites, while the stronger doublets at IS = 0.60−0.64 mm/s are attributed to Fe(II) sites. Thus, the Mössbauer spectra are in agreement with the 6Fe(II)−2Fe(III) oxidation state. Interestingly, the P^N-cluster was reported to exhibit also two doublets in a 1:3 ratio, while their IS parameters of 0.65 and 0.61 mm/s suggest that all iron atoms in the cluster are ferrous.[5]

Comparison of the quadrupole splittings (QS) for **1**, **3a**, and **5** leads to identification of the Fe(III) sites in the clusters. Each of the two doublets of **1** has a QS parameter nearly identical to that of **3a**, and the substitution of $SC(NMe_2)_2$ in **1** by $S(C_6H_4$-4-Me) at the Fe4 and Fe8 sites (see Table 1 for the numbering scheme) hardly affects the QS values. On the other hand, change of the ligand at the Fe1 and Fe5 sites from $N(SiMe_3)_2$ to SBtp affects the QS parameter dramatically for the weaker doublet assigned to Fe(III) centers, while the stronger doublet is intact. The large quadrupole splitting of QS = 1.28 for **1** becomes QS = 0.68 for **5**, the latter of which is as small as those of the stronger doublets for the three model clusters. Therefore, it is reasonable to conclude that the Fe(III) sites in the model clusters are Fe1 and Fe5. Decrease of the QS value, in going from **1** to **5**, can be explained by the different coordination environment of the peripheral iron atoms, because the tetrahedral geometry at these iron centers are more isotropic for **5**, being coordinated by four S donors, than the corresponding coordination for **1**, where three S donors and one N-donor are bound. The reason for the very large quadrupole splittings of two doublets for the P^N-cluster remains unclear. Because the structure and the Mössbauer spectrum are similar between P^N-cluster and the model clusters, and because the peripheral iron centers in the models are assigned as Fe(III), oxidation of the P^N-cluster would occur preferentially at the peripheral iron sites.

The clusters **1**, **3a**, and **5** were found to be EPR silent at 4−100 K, suggesting a diamagnetic ground state. Temperature-dependent magnetic susceptibilities were also measured for crystalline samples of these clusters at 2−300 K, and minor impurity and diamagnetic corrections were applied to the data. Their μ_{eff}-T curves are similar. As the temperature is lowered, the magnetic moment decreases from 0.542−0.575 μ_B per Fe at 300 K and approaches 0.012−0.046 μ_B per Fe at 2−9 K, and the singlet ground state is acertained. Curve fitting of the μ_{eff}-T plots based on standard antiferromagnetic coupling schemes has been difficult, because the [8Fe-7S] core of **1** is a strongly correlated multispin system. However, we reported that the spin structure of **1** was successfully described by broken-symmetry HDFT (hybrid density function theory) calculations and the subsequent spin-projected symmetry-adapted analysis.[26] The theoretical study reproduces well the observed temperature dependence of magnetic moment (μ_{eff}), and indicates that the Fe(III) sites are in fact Fe1 and Fe5.

3. Experimental Section

3.1. General Procedures. All reactions were carried out using standard Schlenk techniques and a glovebox under a nitrogen or argon atmosphere. Toluene, diethyl ether, THF, pentane, hexane, acetonitrile, and hexamethyldisiloxane (HMDSO) were purified by the method of Grubbs,[27] where the solvents were passed over columns of activated alumina and a supported copper catalyst supplied by Hansen & Co. Ltd. Solvents, degassed and distilled from sodium benzophenone ketyl were also used. Infrared spectra were recorded on a JASCO A3 spectrometer. ESI-TOF-MS spectra were recorded on a Micromass LCT TOF-MS at room temperature. UV−vis spectra were measured on a JASCO V560 spectrometer at room temperature. The EPR spectrum was recorded on a JEOL JES-FA200 spectrometer. The magnetic susceptibility was measured using a Quantum Design MPMS-XL SQUID-type magnetometer, and the crystalline samples were sealed in quartz tubes. An impurity correction was made by fitting the data to an equation of the form $\chi_{impurity} = C/T$ at $4 \le T \le 20$ K. The Mössbauer spectrum was measured using a Wissel Mössbauer spectrometer with a ^{57}Co(Rh) source in the constant acceleration mode at 77 K. The crystalline samples were sealed in thin glass tubes, and 3−5 tubes were bundled for the measurements. The spectrum was fitted to Lorentzian lines by least-squares calculations. Velocity calibration was done by measuring the magnetic splitting of α-iron foil. Isomer shifts are referenced to α-Fe at room temperature. Isomer shifts (IS) and quadrupole splitting (QS) are reported in mm/s. Cyclic voltammograms were recorded in THF at room temperature using glassy carbon as the working electrode with 0.2 M $(Bu_4N)(PF_6)$ as supporting electrolyte. The potentials are referenced to Ag/Ag^+.

(26) Shoji, M.; Koizumi, K.; Kitagawa, Y.; Yamanaka, S.; Okumura, M.; Yamaguchi, K.; Ohki, Y.; Sunada, Y.; Honda, M.; Tatsumi, K. *Int. J. Quantum Chem.* **2006**, *106*, 3288–3302.
(27) Pangborn, A. B.; Giardello, M. A.; Grubbs, R. H.; Rosen, R. K.; Timmers, F. J. *Organometallics* **1996**, *15*, 1518–1520.

Elemental analyses were performed on a LECO-CHNS-932 elemental analyzer where the crystalline samples were sealed in silver capsules under nitrogen. X-ray diffraction data were collected on a Rigaku AFC8 or on a Rigaku FR-E equipped with a CCD area detector using graphite-monochromated Mo Kα radiation. See Supporting Information for the details of X-ray crystal structure determination. $Fe\{N(SiMe_3)_2\}_2$,[9] HSTip,[28] $CpFe(C_6H_5S)$,[13] HSBtp,[16] and HSTbt[17] were prepared according to literature procedures. Syntheses of **4**, **7a**, and **7b** were carried out by shielding the solutions from the light because $CpFe(C_6H_5S)$ is moderately light sensitive and gradual formation of an insoluble material was observed upon letting the the solution stand.

We have been unable to obtain satisfactory elemental analyses on **3c**. Single crystals of diffraction quality always gave low values for carbon and sulfur. Either their thermal lability or incomplete combustion is responsible for the unsatisfactory analyses.

3.2. Synthesis of $[\{N(SiMe_3)_2\}\{SC(NMe_2)_2\}Fe_4S_3]_2(\mu_6\text{-}S)\{\mu\text{-}N(SiMe_3)_2\}_2$ (1). A toluene (16 mL) solution of $SC(NMe_2)_2$ (2.85 g, 21.6 mmol) was added to a Schlenk tube containing $Fe\{N(SiMe_3)_2\}_2$ (21.6 g, 57.2 mmol), and then a toluene (24 mL) solution of HSTip (20.3 g, 85.9 mmol) was added. The color of the reaction mixture turned from green to dark brown. Addition of a toluene (90 mL) solution of S_8 (1.61 g, 6.28 mmol) caused further color change to dark purple and then to black. After stirring this mixture for 12 h at 30 °C, the tube was kept standing at room temperature for 10 days. Black needles of $\mathbf{1}\cdot C_7H_8$ were collected, washed with hexane, and dried under vacuum (9.74 g, 5.83 mmol, 82%). UV−vis (toluene): λ_{max} = 254 (ε 48900), 378 (ε 17500) nm. IR (nujol, cm^{-1}): 1600(w), 1465(s), 1388(s), 1365(s), 1311(w), 1230(s), 1180(w), 1083(m), 998(w) 950(w), 923(m), 848(s), 782(w), 755(m), 698(w), 667(w), 615(w). Cyclic voltammogram (1 mM in THF, potential vs Ag/Ag^+): $E_{1/2}$ = −1.29, −1.69 V. Mössbauer spectrum (mm/s, 77 K): IS = 0.61 and QS = 0.54 (77% intensity), IS = 0.37 and QS = 1.28 (23% intensity). EPR (microwave power 0.998 mW; microwave frequency 9055.069 MHz; modulation width 0.1 mT; 4 mM in toluene): Silent in the range of 4−40 K. Magnetic susceptibility (B.M.): μ_{eff}/Fe = 0.023 (2 K), 0.575 (300 K). Anal. Calcd for $C_{34}H_{96}Fe_8N_8S_9Si_8\cdot C_7H_8$: C, 29.50; H, 6.28; N, 6.71; S, 17.29. Found: C, 29.76; H, 6.12; N, 6.59; S, 17.42.

3.3. Synthesis of $Fe_3\{N(SiMe_3)_2\}_2(\mu\text{-STip})_4$ (2). Complex **2** was synthesized according to the literature,[12] while the reported yield of 36% has greatly been improved to 92%, as described below. A toluene (20 mL) solution of HSTip (16.7 g, 70.8 mmol) was added to a Schlenk tube with toluene (30 mL) and $Fe\{N(SiMe_3)_2\}_2$ (20.0 g, 53.1 mmol) at room temperature. After stirring for 30 min, the tube was kept standing at −40 °C for two days. The supernatant was taken out by a syringe to leave black crystals of $\mathbf{2}\cdot C_7H_8$, which were dried under reduced pressure (21.6 g). The black solution was concentrated to half volume, and the second crop (3.07 g) was obtained by cooling the solution at −40 °C. Total amount of $\mathbf{2}\cdot C_7H_8$ was 24.7 g (16.2 mmol, 92%).

3.4. Synthesis of 1 from 2. The synthetic procedure is analogous to that using $Fe\{N(SiMe_3)_2\}_2$ as the precursor. A toluene (15 mL) solution of $SC(NMe_2)_2$ (2.42 g, 18.3 mmol) and HSTip (1.92 g, 8.12 mmol) and a toluene (65 mL) solution of S_8 (1.37 g, 5.32 mmol) were successively added to a toluene (40 mL) solution of $\mathbf{2}\cdot C_7H_8$ (24.7 g, 16.2 mmol). Upon standing this reaction mixture at ambient temperature, black needles of $\mathbf{1}\cdot C_7H_8$ (7.45 g, 4.46 mmol, 73%) were formed.

3.5. Synthesis of $(NEt_4)_2[\{N(SiMe_3)_2\}(SC_6H_4\text{-}4\text{-}Me)Fe_4S_3]_2(\mu_6\text{-}S)\{\mu\text{-}N(SiMe_3)_2\}_2$ (3a). A fluorobenzene (10 mL) suspension of $(NEt_4)(SC_6H_4\text{-}4\text{-}Me)$ (45.0 mg, 0.180 mmol) was added dropwise to a fluorobenzene (20 mL) solution of $\mathbf{1}\cdot C_7H_8$ (150 mg, 8.99 × 10^{-2} mmol) at −40 °C. After stirring for 12 h at −40 °C, the solvent was removed under reduced pressure below 0 °C. The black residue was washed with toluene (15 mL × 2) and was extracted with THF (5 mL). After being centrifuged to remove a small amount of insoluble solid, the THF solution was cooled at −30 °C. Black crystals of **3a** grown from the solution were washed with toluene and dried under vacuum (42 mg, 2.16 × 10^{-2} mmol, 24%). ESI-TOF-MS (THF): m/z = 777.9 ($[M]^{2-}$, 100%), 1690.9 ($(NEt_4)[M]^-$, 23%). UV−vis (THF): λ_{max} = 267 (ε 38000), 370 (ε 23000), 425 (ε 21000) nm. IR (nujol, cm^{-1}): 1600(m), 1465(s), 1388(s), 1365(s), 1230(s), 1170(w), 1083(m), 999(w) 951(m), 848(s), 831(s), 783(w), 756(s), 698(s), 667(w), 615(w). Cyclic voltammogram (1 mM in THF, potential vs Ag/Ag^+): $E_{1/2}$ = −1.76, −2.08 V. Mössbauer spectrum (mm/s, 77 K): IS = 0.60 and QS = 0.56 (75% intensity), IS = 0.38 and QS = 1.30 (25% intensity). EPR (microwave power 0.998 mW; microwave frequency 8955.914 MHz; modulation width 0.1 mT; 5 mM in THF): Silent in the range of 4−40 K. Magnetic susceptibility (B.M.): μ_{eff}/Fe = 0.0124 (8 K), 0.553 (300 K). Anal. Calcd for $C_{54}H_{126}Fe_8N_6S_9Si_8$: C, 35.64; H, 6.98; N, 4.62; S, 15.86. Found: C, 35.85; H, 6.82; N, 4.53; S, 15.69.

3.6. Synthesis of $(NEt_4)_2[\{N(SiMe_3)_2\}(SAr)Fe_4S_3]_2(\mu_6\text{-}S)\{\mu\text{-}N(SiMe_3)_2\}_2$ (Ar = C_6H_4-4-^{t}Bu (3b), C_6H_4-4-Cl (3c), C_6H_4-4-Br (3d), C_6H_4-2-$SiMe_3$ (3e)). The procedure for the synthesis of **3b**−**e** is analogous to that of **3a**.

3.6.1. 3b: The reaction of $\mathbf{1}\cdot C_7H_8$ (150 mg, 8.99 × 10^{-2} mmol) with $(NEt_4)(SC_6H_4\text{-}4\text{-}^tBu)$ (53 mg, 0.180 mmol) gave **3b** as black crystals (50 mg, 2.43 × 10^{-2} mmol, 27%). ESI-TOF-MS (THF): m/z = 820.2 ($[M]^{2-}$, 100%), 1551.0 ($[M] - N(SiMe_3)_2 - S(C_6H_4\text{-}4\text{-}^tBu) + STip$, 23%). UV−vis (THF): λ_{max} = 268 (ε 39000), 360 (ε 23000), 426 (sh, ε 21000) nm. IR (nujol, cm^{-1}): 1589(w), 1459(s), 1390(m), 1367(m), 1299(w), 1241(s), 1180(w), 1076(m), 1010(w) 948(s), 850(s), 781(m), 738(w), 705(w), 665(m), 613(m). Cyclic voltammogram (1 mM in THF, potential vs Ag/Ag^+): $E_{1/2}$ = −1.90, −2.17 V. Anal. Calcd for $C_{60}H_{138}Fe_8N_6S_9Si_8$: C, 37.85; H, 7.31; N, 4.41; S, 15.16. Found: C, 37.64; H, 7.70; N, 4.60; S, 15.43.

3.6.2. 3c: The reaction of $\mathbf{1}\cdot C_7H_8$ (150 mg, 8.99 × 10^{-2} mmol) with $(NEt_4)(SC_6H_4\text{-}4\text{-}Cl)$ (49 mg, 0.180 mmol) gave **3c** as black crystals (89 mg, 4.78 × 10^{-2} mmol, 53%). ESI-TOF-MS (THF): m/z = 799.1 ($[M]^{2-}$, 100%), 790.5 ($[M] - N(SiMe_3)_2 + S(C_6H_4\text{-}4\text{-}Cl)$, 40%), 782.1 ($[M] - 2N(SiMe_3)_2 + 2S(C_6H_4\text{-}4\text{-}Cl)$, 10%). UV−vis (THF): λ_{max} = 272 (ε 44000), 370 (ε 29000), 427 (sh, ε 22000) nm. IR (nujol, cm^{-1}): 1600(m), 1463(s), 1388(s), 1365(s), 1299(w), 1232(s), 1170(m), 1081(m), 1002(w) 946(m), 848(s), 779(w), 755(m), 700(s), 663(w), 615(w). Cyclic voltammogram (1 mM in THF, potential vs Ag/Ag^+): $E_{1/2}$ = −1.79, −2.13 V.

3.6.3. 3d: The reaction of $\mathbf{1}\cdot C_7H_8$ (150 mg, 8.99 × 10^{-2} mmol) with $(NEt_4)(SC_6H_4\text{-}4\text{-}Br)$ (57 mg, 0.180 mmol) gave **3d** as black crystals (114 mg, 5.85 × 10^{-2} mmol, 65%). ESI-TOF-MS (THF): m/z = 843.4 ($[M]^{2-}$, 100%), 858.7 ($[M] - N(SiMe_3)_2 + S(C_6H_4\text{-}4\text{-}Br)$, 30%). UV−vis (THF): λ_{max} = 271 (ε 42000), 370 (ε 27000), 424 (sh, ε 24000) nm. IR (nujol, cm^{-1}): 1600(w), 1463(s), 1388(m), 1365(s), 1230(w), 1170(w), 1081(w), 1002(w) 950(w), 847(m), 779(w), 756(m), 698(s), 667(w), 615(w). Cyclic voltammogram (1 mM in THF, potential vs Ag/Ag^+): $E_{1/2}$ = −1.92, −2.27 V. Anal. Calcd for $C_{52}H_{120}Br_2Fe_8N_6S_9Si_8$: C, 32.04; H, 6.20; N, 4.31; S, 14.80. Found: C, 32.29; H, 5.71; N, 4.11; S, 14.93.

3.6.4. 3e: The reaction of $\mathbf{1}\cdot C_7H_8$ (150 mg, 8.99 × 10^{-2} mmol) with $(NEt_4)(SC_6H_4\text{-}2\text{-}SiMe_3)$ (56 mg, 0.180 mmol) gave **3e** as black crystals (43 mg, 2.07 × 10^{-2} mmol, 23%). ESI-TOF-MS (THF): m/z = 837.0 ($[M]^{2-}$, 29%), 848.0 ($[M] - N(SiMe_3)_2 + S(C_6H_4\text{-}2\text{-}SiMe_3)$, 100%), 858.4 ($[M] - 2N(SiMe_3)_2 + 2S(C_6H_4\text{-}2\text{-}SiMe_3)$, 45%), 1805.8 ($(NEt_4)[M]^-$, 72%). UV−vis (THF): λ_{max} = 272 (ε 34000), 370 (ε 25000), 424 (sh, ε 20000) nm. IR (nujol, cm^{-1}): 1600(w), 1450(s), 1388(s), 1365(s), 1299(w), 1236(s), 1170(m), 1097(m), 998(m) 946(s), 848(s), 781(m), 754(s), 700(s), 665(w), 617(w). Cyclic voltammogram (1 mM in THF, potential vs Ag/Ag^+): $E_{1/2}$ = −1.83, −2.21 V. Anal. Calcd for $C_{58}H_{138}Fe_8N_6S_9Si_{10}$: C, 35.98; H, 7.18; N, 4.34; S, 14.91. Found: C, 36.19; H, 6.85; N, 4.04; S, 14.91.

3.7. Synthesis of $[\{N(SiMe_3)_2\}\{CpFe(C_6H_5S)\}Fe_4S_3]_2(\mu_6\text{-}S)\{\mu\text{-}N(SiMe_3)_2\}_2$ (4). A THF (16 mL) suspension of $CpFe(C_6H_5S)$ (343 mg, 1.49 mmol) was added dropwise to a THF (20 mL) solution of $\mathbf{1}\cdot C_7H_8$ (1.26 g, 0.755 mmol) at −40 °C. After stirring for 15 h

(28) Blower, P. J.; Dilworth, J. R.; Hutchinson, J. P.; Zubieta, J. A. *J. Chem. Soc., Dalton Trans.* **1985**, 1533–1541.

at −40 °C, the solvent was removed under reduced pressure. The black residue was washed with hexane (15 mL × 2), and was extracted with THF/toluene (3:1 v/v, 24 mL). After being centrifuged to remove a small amount of insoluble solid, the solution was transferred to a Schlenk tube and was concentrated to half volume. The tube was covered with aluminum foil and was kept standing at room temperature for a week. Black crystals of **4** grown from the solution were washed with hexane and dried under vacuum (985 mg, 0.555 mmol, 74%). UV−vis (THF): λ_{max} = 271 (ε 25700), 403 (ε 18800) nm. IR (nujol, cm^{-1}): 1601(m), 1466(s), 1389(s), 1366(s), 1230(s), 999(w) 951(m), 926(m), 795(m), 756(s), 699(s), 668(w), 616(w). Cyclic voltammogram (1 mM in THF, potential vs Ag/Ag^+): $E_{1/2}$ = −1.50 V (reversible), E_p^c = −2.13 V (irreversible). Anal. Calcd for $C_{46}H_{92}Fe_{10}N_4S_9Si_8$: C, 31.16; H, 5.23; N, 3.16; S, 16.28. Found: C, 31.22; H, 4.94; N, 3.25; S, 16.37.

3.8. Reaction of 1 with HSTip/SC(NMe$_2$)$_2$. At −78 °C, HSTip (70 mg, 0.31 mmol) was added to a THF (20 mL) solution of **1**·C_7H_8 (0.13 g, 7.79 × 10^{-2}mmol). Then a THF (5 mL) solution of SC(NMe$_2$)$_2$ (30 mg, 0.24 mmol) was added. After stirring the mixture for 2 h at −78 °C, the solvent was removed under reduced pressure. The residue was extracted with toluene (20 mL), and the solution was concentrated to ca. half volume. Black needles of $Fe_4S_4(STip)_2\{SC(NMe_2)_2\}_2$ (64 mg, 5.92 × 10^{-2} mmol, 38%) were obtained from the solution stored at −20 °C. This compound was characterized by comparing the cell parameters of crystals with those reported.[14]

3.9. Reaction of 1 with HSPh/NEt$_3$. Similar to the reaction of **1** with HSTip/SC(NMe$_2$)$_2$, HSPh (50 μL, 0.53 mmol), **1**·C_7H_8 (0.110 g, 6.59 × 10^{-2} mmol), and NEt_3 (40 μL, 0.26 mmol) were treated in THF for 2 h at −78 °C. After removing the solvent under reduced pressure, the residue was extracted with CH_3CN (10 mL), and then an acetonitrile solution of PPh_4Br (0.11 g, 0.26 mmol) was added. The solution was concentrated to ca. half volume. Black crystals of $(PPh_4)_2[Fe_4S_4(SPh)_4]$ (84 mg, 5.73 × 10^{-2} mmol, 43%) were obtained from the solution stored at −20 °C. This compound was characterized by X-ray crystallography.

3.10. Synthesis of [(SBtp){SC(NMe$_2$)$_2$}Fe$_4$S$_3$]$_2$(μ_6-S){μ-N(SiMe$_3$)$_2$}$_2$ (5). A fluorobenzene (12 mL) solution of HSBtp (45 mg, 0.180 mmol) was added dropwise to a fluorobenzene (20 mL) solution of **1**·C_7H_8 (150 mg, 8.99 × 10^{-2} mmol) at −40 °C. After stirring for 12 h at −40 °C, the solvent was removed under reduced pressure below 0 °C. The black residue was washed with hexane (15 mL) and extracted with toluene/hexane (6:1 v/v, 14 mL). After being centrifuged to remove a small amount of insoluble solid, the solution was transferred to a Schlenk tube. Black crystals of **5** were obtained from the solution layered with hexane (35 mg, 1.89 × 10^{-2} mmol, 21%). UV−vis (THF): λ_{max} = 261 (ε 69000), 423 (ε 25000) nm. IR (nujol, cm^{-1}): 1600(w), 1552(s), 1463(s), 1367(w), 1309(w), 1240(s), 1155(w), 1106(m), 935(m) 840(s), 755(s), 698(s), 665(w), 617(w). Cyclic voltammogram (1 mM in THF, potential vs Ag/Ag^+): $E_{1/2}$ = −1.18, −1.51 V. Mössbauer spectrum (mm/s, 77 K): IS = 0.64 and QS = 0.64 (76% intensity), IS = 0.37 and QS = 0.68 (24% intensity). EPR (microwave power 0.998 mW; microwave frequency 8976.226 MHz; modulation width 0.1 mT; 5 mM in THF): Silent in the range of 4−40 K. Magnetic susceptibility (B.M.): μ_{eff}/Fe = 0.046 (9 K), 0.542 (300 K). Anal. Calcd for $C_{46}H_{102}Fe_8N_6S_{11}Si_8$: C, 31.33; H, 5.83; N, 4.77; S, 20.00. Found: C, 30.80; H, 5.71; N, 5.22; S, 20.09.

3.11. Reaction of 1 with HSBtp and (NEt$_4$)(SBtp). A fluorobenzene (10 mL) solution of HSBtp (45 mg, 0.180 mmol) was added dropwise to a fluorobenzene (20 mL) solution of **1**·C_7H_8 (150 mg, 8.99 × 10^{-2} mmol) at −40 °C. A fluorobenzene (10 mL) suspension of (NEt_4)(SBtp) (35 mg, 8.99 × 10^{-2} mmol) was then added to the mixture. After stirring for 12 h at −40 °C, the solvent was removed under reduced pressure below 0 °C. The black residue was washed with hexane (10 mL × 2) and extracted with THF (6 mL). After being centrifuged to remove a small amount of insoluble solid, the solution was transferred to a Schlenk tube. Black crystals of $(NEt_4)_3[(SBtp)Fe_4S_3]_2\{SC(NMe_2)_2\}(SBtp)(\mu_6\text{-}S)\{\mu\text{-}N(SiMe_3)_2\}_2$ (**6**, 2.5 mg, 1.24 × 10^{-3} mmol, 1.4%) were obtained from the solution layered with hexane. UV−vis (THF): λ_{max} = 259 (ε 62000), 348 (ε 29000), 425 (ε 32000) nm. IR (nujol, cm^{-1}): 1600(m), 1542(w), 1463(s), 1388(s), 1365(s), 1311(w), 1259(w), 1230(s), 1180(w), 1133(w), 1107(w), 1093(w), 1006(w), 950(w), 923(w), 831(m), 794(w), 755(s), 700(s), 617(w). Anal. Calcd for $C_{61}H_{131}Fe_8N_5S_{11}Si_{10}$: C, 36.36; H, 6.55; N, 3.48; S, 17.50. Found: C, 36.73; H, 6.59; N, 3.80; S, 17.50.

3.12. Synthesis of [(SBtp){CpFe(C$_6$H$_5$S)}Fe$_4$S$_3$]$_2$(μ_6-S){μ-N(SiMe$_3$)$_2$}$_2$ (7a). At −40 °C, a THF (16 mL) solution of HSBtp (67 mg, 0.263 mmol) was added dropwise to a THF (20 mL) solution of **4** (230 mg, 0.130 mmol). The reaction mixture was stirred for 4 h with warming to room temperature. The solution was concentrated to ca. 9 mL in volume. After being centrifuged to remove the insoluble solid, the solution was transferred to a Schlenk tube. The tube was covered with aluminum foil and was kept standing at room temperature. A crystalline solid of **7a** obtained from the solution was washed with hexane and dried under vacuum (77 mg, 3.93 × 10^{-2} mmol, 30%). UV−vis (THF): λ_{max} = 426 (ε 32800) nm. IR (nujol, cm^{-1}): 1601(m), 1465(s), 1389(s), 1366(s), 1230(m), 999(w) 950(w), 924(w), 795(w), 756(s), 699(s), 667(w), 616(w). Cyclic voltammogram (1 mM in THF, potential vs Ag/Ag^+): $E_{1/2}$ = −1.26, −1.57 V. Anal. Calcd for $C_{58}H_{98}Fe_{10}N_2S_{11}Si_8$: C, 35.56; H, 5.04; N, 1.43; S, 18.00. Found: C, 35.60; H, 5.20; N, 1.10; S, 17.60.

3.13. Synthesis of [(STbt){CpFe(C$_6$H$_5$S)}Fe$_4$S$_3$]$_2$(μ_6-S){μ-N(SiMe$_3$)$_2$}$_2$ (7b). The synthetic procedure is analogous to that for **7a**. The reaction of **4** (136 mg, 8.15 × 10^{-2} mmol) with HSTbt (87 mg, 0.15 mmol) in THF at −40 °C gave **7b**·$(C_6H_{12})_2$, which was crystallized as black plates from THF/cyclohexane (50 mg, 1.79 × 10^{-2} mmol, 22%). UV−vis (THF): λ_{max} = 464 (ε 59000) nm. IR (nujol, cm^{-1}): 1601(w), 1466(s), 1389(s), 1365(s), 1230(s), 999(w) 953(w), 923(w), 795(w), 756(s), 699(s), 616(w). Cyclic voltammogram (1 mM in THF, potential vs Ag/Ag^+): $E_{1/2}$ = −1.33, −1.68 V. Anal. Calcd for $C_{100}H_{198}Fe_{10}N_2S_{11}Si_{16}$: C, 43.06; H, 7.16; N, 1.00; S, 12.65. Found: C, 42.44; H, 6.85; N, 1.16; S, 12.90.

Acknowledgment. This research was financially supported by Grants-in-Aid for Scientific Research (Nos. 18GS0207 and 18064009) from the Ministry of Education, Culture, Sports, Science and Technology, Japan. We thank Roger E. Cramer (the University of Hawaii) for fruitful discussion and careful reading of the manuscript. We also thank Liu Dong (Nagoya Univ.) for helping us to crystallize $(PPh_4)_2[Fe_4S_4(SPh)_4]$. We are grateful to Wataru Fujita, Hirofumi Yoshikawa, and Kunio Awaga (Nagoya Univ.) for aiding us in the SQUID and EPR measurements.

Supporting Information Available: Details of X-ray crystallographic studies of **1**, **3a**−**e**, **4**, **5**, **6**, **7b**, and $(PPh_4)_2[Fe_4S_4(SPh)_4]$ (PDF), and an X-ray crystallographic information file (CIF). This material is available free of charge via the Internet at http://pubs.acs.org.

JA9055036